

Electronic Supplementary Information to

**Assessing the Properties of Supercritical Water in Terms of
Structural Dynamics and Electronic Polarization Effects**

Philipp Schienbein and Dominik Marx

Lehrstuhl für Theoretische Chemie, Ruhr-Universität Bochum, 44780 Bochum, Germany

(Dated: October 14, 2019)

I. CLUSTER SIZE DISTRIBUTIONS

In the main text, we elaborately discuss the cluster size distribution as obtained from the SCW H-bond criterion. To support the statement that this distribution strongly depends on the chosen H-bond criterion we additionally present the distribution as obtained from the RTW H-bond criterion in Fig. S1 (see main text for the definition of both criteria). By comparing the two figures clear differences are unveiled; especially in case of the intermediate states, i.e. 0.4, 0.6 and 0.8 kg L⁻¹, where also qualitatively different conclusions might be drawn from the two distinct H-bond definitions: The more lenient SCW criterion shows that larger cluster sizes containing more than 124 water molecules are populated at 0.6 kg L⁻¹. In contrast, the stricter RTW criterion does not show any larger clusters at that density at all. Recall that there are only 128 molecules in the box and therefore this is the largest possible cluster size. In the same vein, at 1.0 kg L⁻¹ there are almost no monomers according to the SCW criterion, whereas the fluid consists of about 30 % monomers according to the RTW criterion.

The consequences of different geometrical definition of the SCW and the RTW criterion are graphically illustrated in Fig. S2. Clearly, the RTW criterion, which has been shown to be useful several times [1–3], nicely separates the H-bonding feature (1.9 Å, $\cos \Theta = -1$) in the case of liquid ambient water. In contrast, this criterion appears to be too strict in case of supercritical water according to the contours in Fig. S2 which is why we defined the SCW H-bond criterion being more lenient [3]. Importantly, both criteria are reasonable to structurally define H-bonding structures at both, ambient and supercritical conditions, because they both cut through the saddle point region in between the H-bond feature and the remaining configurations.

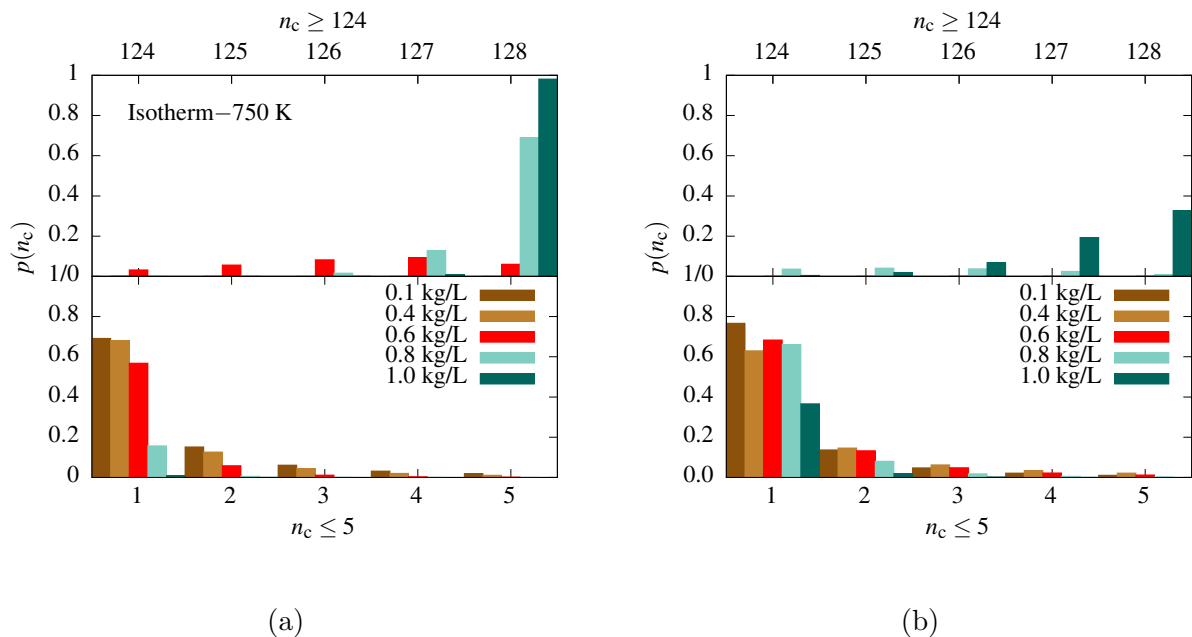


FIG. S1: Probability distribution that a water molecule belongs to a H-bonded cluster (see main text for definition) of total size n_c at 750 K and densities of 0.1 (dark brown), 0.4 (light brown), 0.6 (red), 0.8 (light green), and 1.0 kg L⁻¹ (dark green) as obtained for RPBE-D3 water. Panel (a) and (b) show the distribution as it is obtained using the geometrical SCW and RTW H-bond criteria, respectively. Note that $n_c = 1$ and 2 correspond to the water monomer and dimer, respectively. The distributions are normalized such that $\sum_{n_c} p(n_c) = 1$ at each density. The top panels (with top scale) show all cluster sizes of $n_c \geq 124$, whereas the lower panels (with bottom scale) display the cluster sizes of $n_c \leq 5$; recall that our periodic simulation box contains 128 water molecules in total. Intermediate cluster sizes ($5 < n_c < 124$) are almost not populated and therefore not shown. Note that panel (a) is an exact copy of Fig. 5 in the main text and is reprinted here for convenience.

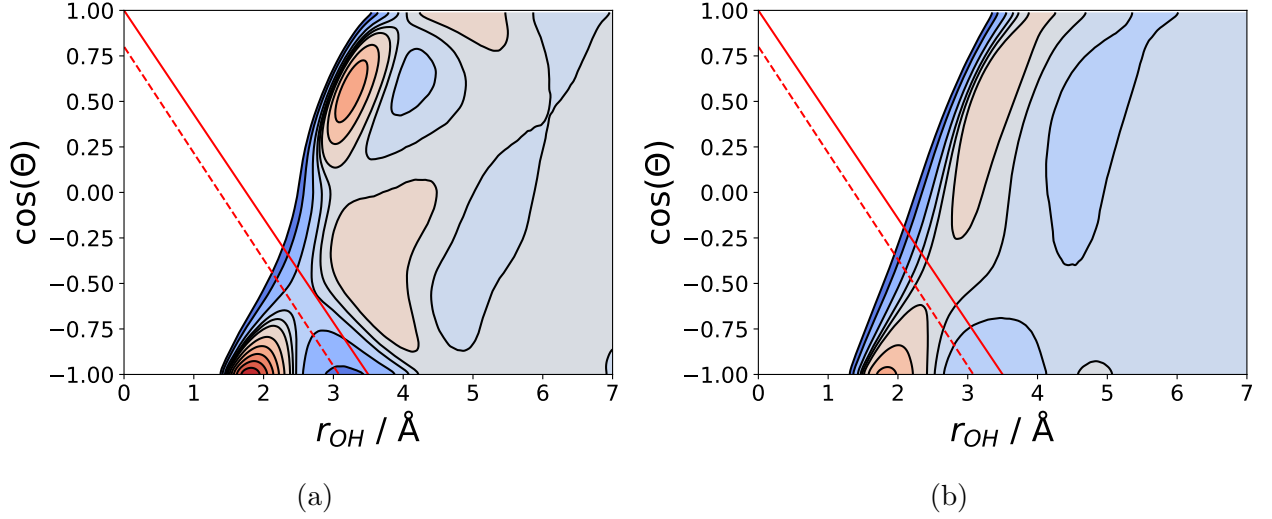


FIG. S2: Joint probability distribution functions of the H-bonding structure of water as described by the intermolecular $\text{O}\cdots\text{H}$ distance r_{OH} and the intermolecular $\text{O}-\text{H}\cdots\text{O}$ angle Θ in case of liquid ambient water (a) and supercritical water at 1.0 kg L^{-1} and 750 K (b) described by the RPBE-D3 density functional. The probability increases from dark blue to dark red colors while white corresponds to zero probability. The contours are shown on a logarithmic scale and the same contour levels are used in both panels to allow for one-to-one comparison. The SCW and RTW H-bond criteria are marked using red solid and dashed lines, respectively. Both criteria are defined according to Eq. (1) in the main text. Note that an angle of 180° ($\cos \Theta = -1$) corresponds to a perfectly linear $\text{O}-\text{H}\cdots\text{O}$ arrangement.

II. FINITE SIZE CORRECTION OF THE SELF-DIFFUSION COEFFICIENT

As discussed in the main text, see Eq. (9) therein, the finite-size corrected self-diffusion coefficient

$$D_0 = D_{\text{PBC}} + \frac{2.837k_{\text{B}}T}{6\pi\eta L} \quad , \quad (\text{S1})$$

is estimated from the system-size dependent self-diffusion coefficient D_{PBC} which is computed throughout using 128 water molecules hosted by a periodic cubic box of length L from Eq. (8) in the main text, where T is the temperature, η the viscosity, and k_{B} is Boltzmann's constant [4, 5].

Both self-diffusion coefficients, D_0 and D_{PBC} , are plotted in Fig. S3 (a) and (b) to disclose the impact of the finite-size correction on the scales set by the thermodynamically induced changes of self-diffusion along isothermal and isochoric pathways. The finite-size correction only leads to a slight increase of the self-diffusion coefficient with respect to the uncorrected value. Still, the correction term increases with increasing temperature. However, the correction is comparably small, especially for the low density states where the self-diffusion coefficient itself becomes very large.

The viscosities at each thermodynamic state point were obtained from the experimental IAPWS95 equation of state [6] and they are shown in Fig. S3 (c) and (d). Note that the temperature of our simulations cannot directly be compared with the experimental temperature (see main text for discussion). Nevertheless we decided to take the viscosities at 750 K, i.e. the nominal simulation temperature, to avoid any arbitrary fudge factors. For sake of different use in the future, we also report the uncorrected D_{PBC} data in the ESI[†].

At 750 K the experimental viscosity shows a kink around 1.0 kg L^{-1} . However, the value at 1.1 kg L^{-1} and 750 K is outside of the validity range of the IAPWS95 equation of state. While extrapolations to higher pressures/densities are generally possible, experimental accuracy is not guaranteed [6]. Therefore, our finite-size corrected self-diffusion coefficient is reported subject to that caveat.

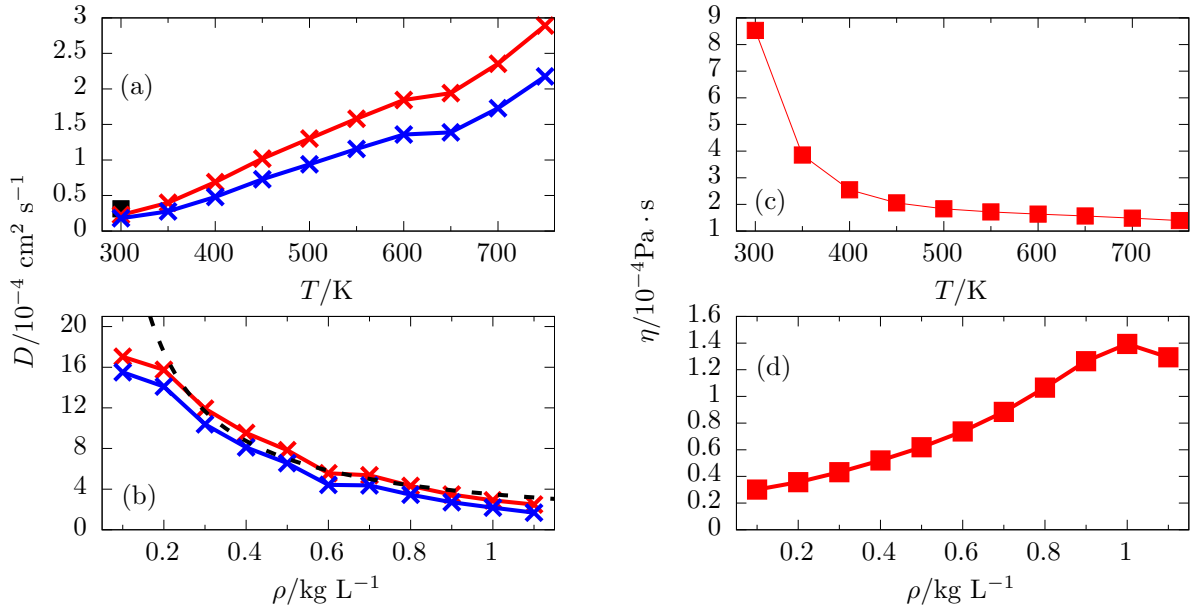


FIG. S3: Self-diffusion coefficients as directly obtained from the simulations in the finite periodic box (D_{PBC} , blue) and their finite-size corrected values (D_0 , red, computed according to Eq. (S1)) of RPBE-D3 water along the isochore at 1.0 kg L^{-1} as a function of temperature (a) and along the supercritical isotherm at 750 K as a function of density (b). The dashed line represents the experimental fit based on NMR data [7] that is depicted here without adjustments. The filled square marks the self-diffusion coefficient of $\approx 0.3 \times 10^{-4} \text{ cm}^2 \text{ s}^{-1}$ for ambient liquid water at its experimental density computed from neural network molecular dynamics simulations of RPBE-D3 water [8]. Panel (c) and (d) depict the viscosity according to the experimental IAPWS95 equation of state [6] at 1.0 kg L^{-1} as a function of temperature and at 750 K as a function of density, respectively. These values are used to correct for the finite size of our simulation box according to Eq. (S1); note that the value at 1.1 kg L^{-1} and 750 K is outside of the validity range of the equation of state (see text).

-
- [1] S. Imoto, H. Forbert, and D. Marx, *Phys. Chem. Chem. Phys.* **17**, 24224 (2015).
- [2] P. Schienbein, G. Schwaab, H. Forbert, M. Havenith, and D. Marx, *J. Phys. Chem. Lett.* **8**, 2373 (2017).
- [3] P. Schienbein and D. Marx, *J. Phys. Chem. B* **122**, 3318 (2018).
- [4] B. Dünweg and K. Kremer, *J. Chem. Phys.* **99**, 6983 (1993).
- [5] I.-C. Yeh and G. Hummer, *J. Phys. Chem. B* **108**, 15873 (2004).
- [6] W. Wagner and A. Pruß, *J. Phys. Chem. Ref. Data* **31**, 387 (2002).
- [7] W. J. Lamb, G. A. Hoffman, and J. Jonas, *J. Chem. Phys.* **74**, 6875 (1981).
- [8] T. Morawietz, A. Singraber, C. Dellago, and J. Behler, *Proc. Natl. Acad. Sci. U.S.A.* **113**, 8368 (2016).